8-2015

Estimation of Historic Flows and Sediment Loads to San Francisco Bay, 1849 – 2011

Hamed Moftakhari Rostamkhani
Portland State University, hamed2@pdx.edu

David A. Jay
Portland State University

Stefan A. Talke
Portland State University, talke@pdx.edu

David H. Schoellhamer
United States Geological Survey

Citation Details

Moftakhari, H. R., Jay, D. A., Talke, S., Schoellhamer, D. H., (2015). Estimation of historic flows and sediment loads to San Francisco Bay, 1849–2011. Journal of Hydrology. Volume 529, Part 3, Pages 1247–1261.

Journal of Hydrology 529 (2015) 1247–1261

Contents lists available at ScienceDirect

Journal of Hydrology

journal homepage: www.elsevier.com/locate/jhydrol

Estimation of historic flows and sediment loads to San Francisco Bay, 1849–2011

H.R. Moftakhari [a,*], D.A. Jay [a], S.A. Talke [a], D.H. Schoellhamer [b]

[a] Department of Civil and Environmental Engineering, Portland State University, P.O. Box 751, Portland, OR 97207-0751, USA
[b] United States Geological Survey, 2130 SW 5th Avenue, Portland, OR 97201, USA

ARTICLE INFO

Article history:
Received 27 February 2015
Received in revised form 16 July 2015
Accepted 20 August 2015
Available online 28 August 2015
This manuscript was handled by Konstantine P. Georgakakos, Editor-in-Chief, with the assistance of Marco Toffolon, Associate Editor

Keywords:
Historic sediment load
Discharge estimation
Downscaling
San Francisco Bay
Basin-scale system change
Seasonality

SUMMARY

River flow and sediment transport in estuaries influence morphological development over decadal and century time scales, but hydrological and sedimentological records are typically too short to adequately characterize long-term trends. In this study, we recover archival records and apply a rating curve approach to develop the first instrumental estimates of daily delta inflow and sediment loads to San Francisco Bay (1849–1929). The total sediment load is constrained using sedimentation/erosion estimated from bathymetric survey data to produce continuous daily sediment transport estimates from 1849 to 1955, the time period prior to sediment load measurements. We estimate that ~55% (45–75%) of the ~1500 ± 400 million tons (Mt) of sediment delivered to the estuary between 1849 and 2011 was the result of anthropogenic alteration in the watershed that increased sediment supply. Also, the seasonal timing of sediment flux events has shifted because significant spring-melt floods have decreased, causing estimated springtime transport (April 1st to June 30th) to decrease from ~25% to ~15% of the annual total. By contrast, wintertime sediment loads (December 1st to March 31st) have increased from ~70% to ~80%. A ~35% reduction of annual flow since the 19th century along with decreased sediment supply has resulted in a ~50% reduction in annual sediment delivery. The methods developed in this study can be applied to other systems for which unanalyzed historic data exist.

1. Introduction

Sediment supplied to estuaries and the coastal zone impacts primary production, recreational and commercial fishing, nutrient supply, habitat restoration, human health, the fate and transport of pollutants, geomorphic evolution, and navigation (Fisher et al., 1982; Yang et al., 2003; Schoellhamer et al., 2007; Sherwood et al., 1990). Climate change and watershed management practices modulate runoff and, therefore, the timing and magnitude of sediment delivery to estuaries (Syvitski et al., 2005; Wang et al., 2007; Ganju and Schoellhamer, 2009; McCulloch et al., 2002; Thrush et al., 2004). Processes such as tidal currents, the spring-neap cycle, coastal upwelling, wind waves, watershed inflow and climatic variability cause suspended sediment concentration (SSC) to vary in time and space (Allen et al., 1980; Gelfenbaum, 1983; Pejrup, 1986; Vale and Sundby, 1987; Powell et al., 1989; Ruhl et al., 2001; Orton and Kineke, 2001; Chen et al., 2006; Ralston and Stacey, 2007; Talke and Stacey, 2008). These processes act on multiple time scales, from seconds to years, and have diverse effects on SSC (Schoellhamer, 2002).

Coastal and estuarine processes (e.g. reversing tidal flow, the compensation flow for the tidal Stokes drift, spring-neap water storage effects, and lateral circulation) make the lower reaches of a tidal river a difficult location in which to determine net freshwater discharge and sediment transport. While previous studies have introduced methods to calculate discharge in tidal rivers far from the mouth (Hoitink et al., 2009; Sassi et al., 2011; Kawanisi et al., 2010), it remains challenging to estimate net discharge or transport near the mouth of an estuary with conventional technology (Jay et al., 1997; Fram et al., 2007). Recent studies have proposed methods to estimate river flow using tidal properties, but are limited by coarse time-resolution (Moftakhari et al., 2013), and do not consider the effects of mixed diurnal and semidiurnal tides (Cai et al., 2014).

San Francisco (SF) Bay, used here as a case study, consists of two distinct sub-estuaries. The northern reach, is partially mixed and dominated by seasonally varying fresh water inflows, while the southern part is a well-mixed tidal-lagoon estuary (Cheng and Gartner, 1985; Chua and Fringer, 2011). Freshwater inflow occurs primarily from the Sacramento and San Joaquin rivers (Fig. 1), with

* Corresponding author.
E-mail addresses: hamed2@pdx.edu (H.R. Moftakhari), djay@pdx.edu (D.A. Jay), talke@pdx.edu (S.A. Talke), dschoell@usgs.gov (D.H. Schoellhamer).

http://dx.doi.org/10.1016/j.jhydrol.2015.08.043
0022-1694/

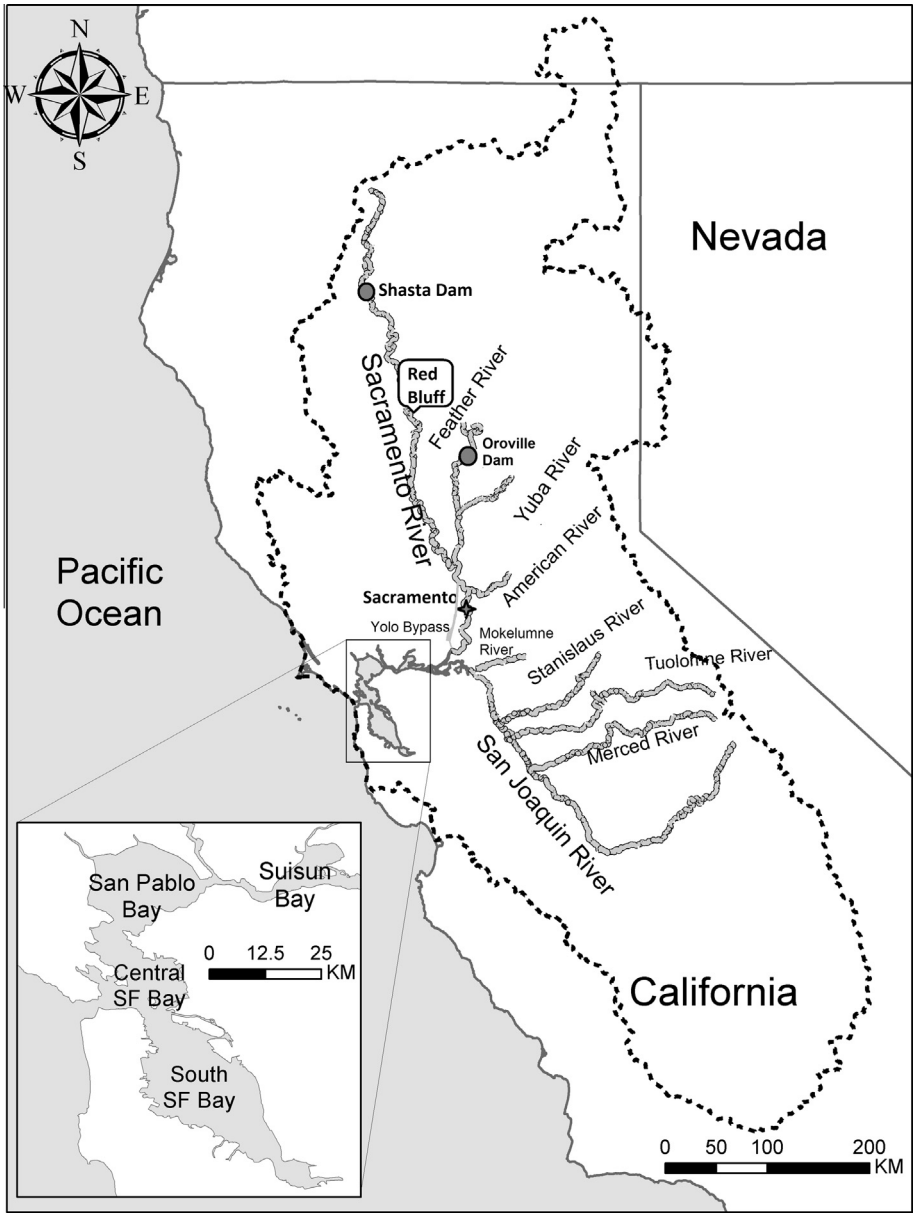

Fig. 1. San Francisco Bay study area and the eight rivers used for the Eight-River-Index drain the Central Valley through SF Bay to the Pacific Ocean; dashed-line shows the boundary of watershed.

annual average flows of 492 $m^3 s^{-1}$ and 41.9 $m^3 s^{-1}$ between 1980 and 2013, respectively (http://wdr.water.usgs.gov/). Flows in both systems have been reduced and altered considerably by diversion (Kimmerer, 2002). Tides in SF Bay have a mixed diurnal–semidiurnal character. The present amplitude of the major semidiurnal constituent M_2 at the Golden Gate is 0.57 m, while the largest diurnal constituent K_1 has an amplitude of 0.37 m (Moftakhari et al., 2013). Coupled with marked daily, seasonal and interannual variability of freshwater inflow, and anthropogenic alterations in wetland coverage, channel depth, and levee heights, SF Bay is a challenging location for analyzing sediment transport processes (Barnard et al., 2013). Nonetheless, the availability of well-defined estuarine boundaries, digitized bathymetric data extending to the mid-19th century, recently re-discovered and processed historic river and tide data (Talke and Jay, 2013), and modern analysis techniques provide the possibility of improving our knowledge of the past system trajectory and the effects of human interventions.

The dynamics of sediment supply to SF Bay are highly variable (Schoellhamer, 2002; Ruhl et al., 2001; Talke and Stacey, 2003, 2008) and difficult to quantify, in addition to the issues posed by river discharge determination. Sediment discharge data for key sub-basins are lacking and the sediment trapping characteristics of upland dams, flood control channels, sediment catch basins, and freshwater tidal marsh components are poorly characterized. In addition, sediment removal is poorly documented, and multiple natural and human alterations have occurred over time (McKee et al., 2013).

A number of studies have estimated the total load or suspended sediment load in SF Bay since 1850 (Gilbert, 1917; Smith, 1965; Porterfield, 1980; McKee et al., 2006, 2013; Ganju et al., 2008; Schoellhamer, 2011). These studies describe how a huge volume of debris was washed into SF Bay in the late 19th and early 20th century by hydraulic and placer mining activities which occurred between the 1850s and 1884. More recently, trapping of sediment

in reservoirs, channel stabilization, flood protection measures, and altered land-use have caused sediment import from the Central Valley to decrease (Jaffe et al., 2007; McKee et al., 2006; Wright and Schoellhamer, 2004). Retrospective studies of sediment loading, beginning with Smith (1965), are based on proxies for daily river flow and/or an assumption that sediment loading characteristics have remained stationary. Neither the 19th century river gauge record from Sacramento (starting in 1849) nor the tidal record from San Francisco (from 1854) have been employed in previous studies. Thus, an opportunity exists to improve our understanding of historical loading and the system response to loading. Because annual discharge has decreased by an estimated 30% since the 19th century (Moftakhari et al., 2013), it is likely that both altered hydrology and changed sediment supply contribute to the changing sediment dynamics in SF Bay.

Long-term trends in SF Bay sediment loading have been inferred by differencing successive historic bathymetric charts (Gilbert, 1917; Fregoso et al., 2008; Ganju et al., 2008; Jaffe et al., 2007; Dallas and Barnard, 2011). Schoellhamer (2011) compared successive bathymetric surveys presented by Cappiella et al. (1999), Fregoso et al. (2008), Foxgrover et al. (2004), and Jaffe et al. (1998) and estimated the changes in bed sediment volume in four sub-embayments of SF Bay (Central SF Bay, South SF Bay, Suisan Bay, and San Pablo Bay; Fig. 1) from the 1850s to the 1980s. Prior to 1855, SF Bay and its watershed are thought to have been relatively undisturbed, although Spanish and Mexican livestock grazing practices produced widespread erosion in local watersheds beginning in the late 18th century (Schoellhamer, 2011; Booker, 2013). Hydraulic mining debris increased bed sediment volume by at least 260 Mm^3 (10^6 m^3) in the late 1800s, almost entirely in Suisun and San Pablo Bay. Significant timber harvest occurred in the Sierra Nevada in support of mining but also for railroad construction and other industrial activities pre-1900 (Burns, 1972; Laudenslayer and Darr, 1990), and may have contributed to sediment loads. There was little change in total bed sediment volume from 1892 to 1925, but Bay's sediment volume increased again by 160 Mm^3 between the 1926 and 1949. This second pulse of sediment has been attributed to urbanization or increased agricultural land use (Schoellhamer, 2011), though a large increase in clear-cutting activity about 1940 (Burns, 1972; Laudenslayer and Darr, 1990) may have also contributed to renewed sediment supply to the Bay. The period from the 1950 to the present has been characterized by erosion and loss of bed material (Schoellhamer, 2011). Diminishment of the hydraulic mining and urbanization sediment pulses, sediment trapping behind dams and in flood bypasses, and bank protection all contribute to decreased sediment supply to the Bay (Schoellhamer, 2011; Singer et al., 2008). The erodible pool of sediment in the Bay was largely depleted by the late 1990s, and produced a step decrease (36%) in SSC from Water-Years (WY) 1991–1998 to 1999–2007 in SF Bay (Schoellhamer, 2011). In summary, SF Bay experienced net deposition from the 1850s to 1950s and net erosion after the mid-20th century (Barnard et al., 2013).

The time period from 1849 to 1946, for which we use observed water level at Sacramento to estimate discharge (see Section 3), can be divided into at least three periods. Before the 1862 floods and the onset of flood protection measures (i.e. channelizing and building levees), the delta system was much less perturbed by human alteration (Booker, 2013) than during later periods, though slow adjustments to tectonic changes or climate shifts were likely occurring. Anthropogenic sources of sediment appear to have been negligible compared to natural processes, and levees were too low to confine the flow within the main channels during large flow events. However, the lack of large floods between 1853 and 1862 produced a time lag between mining activities and sediment flux to the delta (James, 2006, 2010). Flood levees in Sacramento were increased from their pre-1862 height of 7.3 m (Logan, 1872) up to 9.1 m by the 1890s, using hydraulic mining debris (Booker, 2013). During this time, flow confinement by the system of levees and aggradation of the main channel strongly affected the hydraulic characteristics of the system, such that tides ceased to propagate to Sacramento (Gilbert, 1917). Because an increase in friction produces a higher stage (water level) and smaller tide for the same river flow and geometry (Jay et al., 2011), we infer that tidal damping likely occurred due to increased hydraulic roughness in a shallower channel. By the beginning of the third period in 1930, most of the sediment pulse from hydraulic mining activities had moved out of the river channel and into the estuary (Schoellhamer, 2011; James, 2006). Compared to the pre-Gold Rush situation, the primary differences affecting system hydraulics were flow confinement by the system of levees and the loss of wetland floodplains. Channel infill and levee construction after 1862 affected the system in at least two ways. Increased bed elevation raised the observed stage for all flows (Gilbert, 1917), but also altered the range of possible stage heights. Moreover, increased levee heights confined the flow to the channels and produced larger rises in river stage, for the same flow. However, levees often failed upstream of the Sacramento gauge, causing frequent flooding and affecting the river stage downstream (Rose et al., 1895).

There are strong seasonal variations in discharge and sediment transport to SF Bay. At present, about 90% of the precipitation and more than 80% of watershed sediment transport occurs during the wet season between December and April (Conomos and Peterson, 1977; Ganju et al., 2008; Lewicki and McKee, 2010; McKee et al., 2006, 2013). This seasonally focused supply occurs because the major portion of total annual load is transported by high flow periods of limited duration. However, because flow seasonality has changed considerably since 1900 (Moftakhari et al., 2013), we investigate here whether the historical seasonality of sediment loading has also changed.

The fraction of sediment load contributed by local SF Bay tributaries has increased through time, compared to the Sacramento-San Joaquin rivers system (Lewicki and McKee, 2010). Prior to 1955, the sediment load from Central Valley was reported as approximately 89–92% or 85.5% of the total load (Ogden Beeman and Associates, 1992; Smith, 1965). Krone (1979) reported that in 1960, 76% of the total load of SF Bay was from the Central Valley, and estimated that this ratio would decrease to 63% in 1990 and 54% by 2020. More recent studies suggest that local tributaries currently provide 7% of annual inflow, but account for ~60% of the suspended sediment (McKee et al., 2013, 2006). This reflects the effect of dams that block sediment load from 48% of the watershed, flow diversion, and regulation of peak flows (Minear, 2010). By contrast, local, urbanized tributaries exhibit amplified precipitation-discharge characteristics (McKee et al., 2013).

There remains significant uncertainty regarding the history of sediment loading to SF Bay, despite previous work. How has the daily flow and sediment load to SF Bay changed over the last 160 yrs? What are the relative contributions of anthropogenic effects and natural processes to the total sediment budget? Can available archival data be used to improve daily estimates? A method is needed to hindcast flow and sediment input with higher resolution in time, to provide a better understanding of the changes in inputs and related adjustments. In this study we have re-discovered and digitized ~80 years of Sacramento River daily water level data between 1849 and 1946 from which river discharge is estimated after adjusting for changes to the river channel. This discharge measure, which we call the Sacramento Discharge Estimate (SDE), is combined with the Net Delta Outflow Index (NDOI) estimates (1930–2011) and flow estimates from tidal data (1858–2011, downscaled to daily) to provide a more accurate

version of SF Bay historic daily inflows from 1849 to 2011. This Composite Discharge Estimate (CDE), which is the first instrumental estimate of daily delta inflows to SF Bay from 1849 to 1930, is then used, with integral constraints from observed SF Bay bathymetric change, to provide estimates of daily sediment discharge. These discharge estimates are used to describe how the timing and magnitude of sediment import into SF Bay has changed over time. The proposed methodology, using new information of sediment change from bathymetric surveys to constrain sediment load, improves upon previous efforts in time-resolution and accuracy.

2. Setting, data sources and methods

2.1. Data sources

2.1.1. Observed water level of Sacramento River, 1849–2011

River stage measurements began in Sacramento, CA in September 1849 (Logan, 1872; Gilbert, 1917), but the 19th century data have not been evaluated in nearly a century, likely because of calibration difficulties caused by hydraulic mining debris and anthropogenic alterations to the flood control system. Nonetheless, because the stage measurements in Sacramento integrate flow from a catchment basin of about 67,000 km^2 from the states of California, Nevada, and Oregon (Fig. 1), its use as a proxy for Delta outflow from 1849 to 1929 is potentially useful in reconstructing historical sediment loads. In this contribution we have recovered and digitized flow hydrographs from pioneer physician Thomas M. Logan from CA State Library via L. Hunsacker (Logan, 1872; Hunsaker and Curran, 2005) to obtain daily estimates of river stage between WY1850 and WY1862. Daily tabulations of river flow from 1881 to 1892 were recovered and digitized from US Signal Service records (https://www.ncdc.noaa.gov/EdadsV2). Further data from 1893 forward were measured and documented by the US Weather Bureau (USWB) in a series of reports entitled "*Daily river stages at river gage stations on the principal rivers of the United States*". Extreme flood crest stages are listed starting in 1907. It is likely that a staff gauge was maintained between 1862 and 1881, because the Signal Service gauge (1881–1892) retained low water from 1849 as their gauge zero. Moreover, annual peak water levels for WY1874–1881 (State of California, 1889) and estimates of average monthly river discharge and peak annual discharge for WY1878–1884 are available (State Engineering Department of California, 1886). The history of measurements in Sacramento is described by Conner (2005). However, original records for the WY1863–1881 period have not yet been found, requiring that we augment this period using estimates of discharge obtained from the SF tide gauge (Moftakhari et al., 2013). The digitized observed water levels at Sacramento since 1849 are provided in the Supplementary material.

The Sacramento gauges were located until 1979 in Old-Town Sacramento (USGS 11447500), at or near the present day location of the I-Street gauge operated by the California Department of Water Resources (http://cdec.water.ca.gov/cgi-progs/queryF?IST). Prior to 1900, gauge zero was set to the low water mark of 1849 (~1.5 m above the early 20th century mean sea level (MSL) datum, according to USWB 1947). From 1900 to 1913, the zero was shifted to the low-water mark of October 23rd, 1856 (0.15 m below MSL), and since 1914 the zero has been considered equal to MSL of that period. Levee heights before 1862 were 7.3 m (24 feet) above gauge zero (Logan, 1872). After the catastrophic flooding in 1862, levee heights were progressively increased and the flood danger level in 1893 was considered to be at 7.6 m (25 feet), while in 1940s, flood stage was specified to be at 8.8 m (29 feet) (USWB, 1875 to 1947). Available records suggest that the 1.2 m rise in flood stage is primarily the result of increased levee heights and flow confinement (James and Singer, 2008).

2.1.2. Discharge data

This study uses the Net Delta Outflow Index (NDOI) available from WY1930–present (http://www.water.ca.gov/dayflow/) as a proxy for tidally averaged daily river inflow to SF Bay from the Sacramento River delta. NDOI represents about 93% of the inflow to SF Bay, and accounts for river inflow, precipitation, evaporation, agricultural consumptive demand, and water exports from the Delta (Conomos and Peterson, 1977). Because Shasta Dam came on-line in the mid-1940s and altered the hydrograph, we use the less anthropogenically altered data from 1930 to 1946 to develop a regression between Sacramento River stage and NDOI. This regression can then be applied to archival stage measurements to obtain an estimate of historic NDOI. However, because fewer stream gauge sites were in place before 1956, NDOI estimates for 1930–1955 are less certain than those for later periods (Moftakhari et al., 2013).

For time periods without river stage measurements (September 1st, 1862–February 24th, 1879, March 28th, 1879–August 31st, 1880, and May 1st, 1888 to December 1st, 1890), we use the ~18-day averaged estimates of NDOI obtained from the historic SF Bay tide gauge from 1858 to 1929 (Moftakhari et al., 2013); these are downscaled to daily, as described below.

2.1.3. Sediment load data

We use the sum of daily sediment load data, available for the Sacramento River at Freeport (USGS 11447650) (http://waterdata.usgs.gov/usa/nwis/uv?site_no=11447650) and the San Joaquin River near Vernalis (USGS 11303500) (http://waterdata.usgs.gov/ca/ nwis/uv/?site_no=11303500) from 1956–present, to validate our proposed approach.

2.1.4. Other data

For validation, our daily flow estimates are compared to the following hydrologic quantities:

(I) *The Eight-River Index (ERI):* Published by The California Department of Water Resources (http://cdec.water.ca.gov/cgi-progs/iodir/WSIHIST), the ERI combines the flows into the Sacramento Delta from the Sacramento and San Joaquin Rivers with major tributaries, including the Feather, Yuba, American, Stanislaus, Tuolumne, and Merced Rivers (Fig. 1), after removing the effect of diversions, storage, export, and import. Monthly totals are available during the wet season (December–May) from 1906 to the present (Ganju et al., 2008).

(II) *The Six River Index (SRI):* The State Engineering Department of California (1886) published monthly mean flow records, from November 1878 to October 1884, for the six principal rivers that drain from the Central Valley to SF Bay. These records include flows for the Sacramento River at Collinsville, CA, the San Joaquin River at Hamptonville, CA, and the Mokelumne, Stanislaus, Tuolumne, and Merced Rivers (Fig. 1).

(III) *Daily Sacramento River discharge at Red Bluff:* Daily discharge data are available at Red Bluff, CA from 1891 to the present (USGS 1377100) and extremes are available back to 1879. Though these data provide the longest independent data set for comparison with our flow estimates, the drainage basin area at Red Bluff (~23,000 km^2) is only 14% of the area at Sacramento.

(IV) *Monthly rainfall totals at Sacramento:* These data are available from the Global Historical Climatology Network of the National Climatic Data Center (http://www.ncdc.noaa.gov/). These data are composed of monthly surface station measurements, and began in January, 1850 for Sacramento (Ganju et al., 2008). They provide the most comprehensive comparison in terms of time period, but are also the least direct.

All the data used in this study are listed in a Supplementary table (see the Supplementary material).

2.2. Methods

2.2.1. Water level adjustment and estimating a stage-discharge rating curve

We use the daily WL data described in Section 2.1.1 to estimate NDOI from 1849 to 1946, but these data must be processed to adjust for system changes.

Fig. 2a displays the observed daily WL time series described in Section 2.1.1. The lowest observed WL each year remains near zero in the 1850s, but increases after 1862 to a maximum of 2.9 m above MSL in 1892. Between the 1890s and 1930, low WL returns to its original, pre-1862 level. The rise before 1892 presumably occurred due to sedimentation from hydraulic mining activities; although hydraulic mining was outlawed in 1884, aggradation continued for nearly a decade thereafter (Gilbert, 1917). This change in lowest observed WL, which approximately represents the change in channel-bed elevation, is known as the Gilbert Wave (James, 2006). Fig. 2a suggests that sedimentation occurred more rapidly (1862–1892) than erosion (1892–1930). Due to this asymmetric curve, we fit the time variation of the bed (H_{bed}) using a log-normal distribution curve

$$H_{bed}(t) = \frac{1}{t\sigma_{bed}\sqrt{2\pi}} e^{-\frac{(\ln[t]-\mu_{bed})^2}{2\sigma_{bed}^2}}, \quad (1)$$

and find that a location parameter (μ_{bed}) and standard deviation (σ_{bed}) of 1892 and 15 yrs, respectively, describe the low WL variation in time. Fig. 2b compares our estimates for temporal low WL variation to the values tabulated by Gilbert (1917) and the State of California (1889). Interannual variations in minimum discharge largely explain the fluctuation of the values around the smooth fit. To obtain a time series of river stage relative to the river bed, we subtract Eq. (1) from the observed WL.

Bed aggradation, changes to levee heights, wetland reclamation, and the development of managed floodplains such as the Yolo Bypass (Fig. 1) greatly altered not only the height of the bed, but also the annual variability in river stage. Before 1862, WL varied between zero and 7.5 m under undisturbed conditions. By the 1880s, the range shrank, and WL varied between about 2 and 8 m. By 1930, the channel bed returned to its pre-1862 level and WL ranged between zero and 9 m above gauge zero. Because insufficient information exists to model in detail changes to the stage/flow relationship over time and to adjust for changing friction, we make statistically-based corrections to the data set and check the corrections ex-post-facto via an independent data set (the tidally-based TDE and the hydrologic data from Section 2.1.4). Therefore, we scale the data before 1930 such that the range is the same as from 1930 to 1944, the calibration period. Because the independently derived TDE flow estimates suggest that the pre-1930 period contained a similar range of flows as the 1930–1944 period (Moftakhari et al., 2013), this assumption appears to be justified. We use two different scaling functions to adjust the measured stage:

(i) An adjustment for 1881–1930 data is made as follows. First, a rating curve from 1879 (Rose et al., 1895) indicates that an increase from low (~300 $m^3 s^{-1}$) to high (~2700 $m^3 s^{-1}$) river discharge caused the WL to rise from 3.7 to 10.7 m in 1879 (Fig. 3a). By contrast, the same variation in river discharge in the 1930s produced a WL range of 1.5–10.1 m (Fig. 3a). Thus, the WL range was ~23% larger in the 1930s compared to 1879. Assuming that hydrologic properties changed gradually over time, we use a log-normal scale function (Sc_r) as:

$$Sc_r(t) = \frac{1}{t\sigma_r\sqrt{2\pi}} e^{-\frac{(\ln[t]-\mu_r)^2}{2\sigma_r^2}}, \quad (2)$$

with the location parameter (μ_r) and standard deviation (σ_r) of 1892 and 15 yrs, respectively, to adjust WL range for 1880–1930 to be comparable to the 1930–1944 period (Fig. 2c). The annual WL range was then adjusted with the scale function to normalize the data, for comparison with the 1930–1944 period. The net result of the adjustments related to the bed elevation and the range scale function is:

$$WL_{adj}(t) = Sc_r(t) \times [WL_{obs}(t) - H_{bed}(t)], \quad (3)$$

where WL_{adj} is the adjusted WL, WL_{obs} is the observed WL, H_{bed} is the log-normal curve describing the variation of bed elevation with time (Fig. 2b) and Sc_r is the range adjustment scale (Fig. 2c).

(ii) The adjustment for 1849–1862 is made as follows. Building levees after 1862 produced a larger WL range in the 1930s, relative to pre-1862 conditions. To adjust the 1849–1862

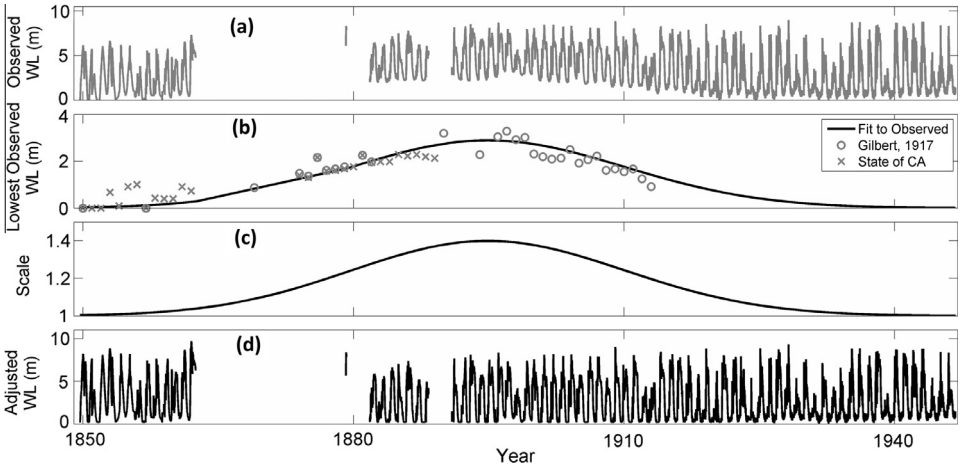

Fig. 2. Panel (a): daily observed Sacramento water level (WL) variation, 1849–1949. Panel (b): variation of annual minimum WL with time. Panel (c): WL range adjustment scale. Panel (d): Adjusted WL for the effects of sedimentation and/or leveeing, with reference to 1930s.

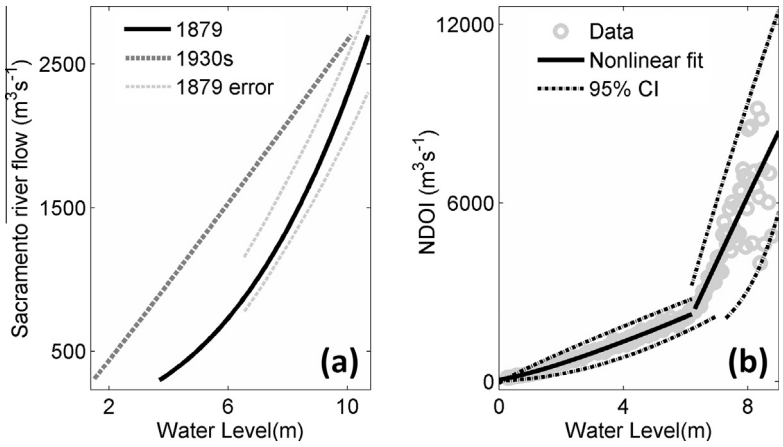

Fig. 3. Panel (a): Calibrated Discharge-WL rating curve at Sacramento, CA during the peak of hydraulic mining activities (solid line) vs dredged channel fifty-years later (dash-dot line). Panel (b): WL-NDOI rating curve calibrated to daily data over 1930–1944.

WL data, we match WY1859–1860 with WY1934–1935, since for both the TDE is available, a similar number of moderately large flow events occurred, and total annual rainfall at Sacramento was similar (within ~10%). From these water years a statistical correlation is developed between tidally based (TDE) flow estimates and observed WL. This analysis shows that the standard deviation for WL observed over WY1859–1860 was, for approximately similar hydrologic events, 30% lower than WY1934–1935. Thus, we scale the 1849–1862 WL by 1.3 before applying the 1930–1944 rating curve (described in Section 2.2.2).

Fig. 2d shows the adjusted WL after all the adjustments mentioned above. Later we check the delta outflow estimate resulting from the adjusted data set against other estimates of flow, where available.

2.2.2. Discharge estimation

We next develop an historic estimate of daily NDOI from 1849 to 1929 using the adjusted water level measured on the Sacramento River (Fig. 2d). A stage-discharge rating curve between NDOI and WL data for WY1930–1944 is first determined, using a least squares fit with the form of $WL = \alpha + \beta \times NDOI^{\gamma}$ which is then applied to 100 evenly spaced bin-averaged flows and water levels (Fig. 3b). During this time period, delta outflow was not significantly altered by flow regulation (reservoirs) or water diversion projects (Barnard et al., 2013). Clearly, the data below and above 6.2 m have a different relationship with discharge. Thus, we divide the data into two subsets (<6.2 m and >6.2 m) and fit the nonlinear curve to each subset, separately. The change in slope above 6.2 m might be due to flooding of the Yolo Bypass floodplain upstream of Sacramento, using weirs that were completed between 1916 and 1934 (Russo, 2010). Before this time period, flooding of this floodplain often occurred (Rose et al., 1895) due to levee breaches or overtopping.

The rating curve in Fig. 3b is then used to convert the adjusted observed WL to SDE during periods for which WL data are available (e.g. 1849–1862, 1879, 1881–1888, and 1891–1929).

2.2.3. Temporal downscaling of tidal discharge estimates

As shown in Fig. 2, there are three gaps in daily observed WL data from 1862 to 1891: (a) September 1862 to February 1879, (b) March 1879 to August 1881, and (c) May 1888 to December 1890. These gaps were filled by TDE (Moftakhari et al., 2013), an approximately 18-day average flow estimate based on tide gauge data (Fig. 4). The time resolution of TDE is set by the harmonic analysis used to produce the TDE estimates (Moftakhari et al., 2013). The 18-day averaged TDE is first linearly interpolated to daily values (TDE_{1d}). Then, a statistical relationship between an 18-day average and the daily peak flow during a flood was found using 31 high-flow events ($TDE_{18d} > 3500\ m^3\ s^{-1}$) between 1930 and 2011, yielding the following relationship between the peak daily NDOI and 18d averaged TDE:

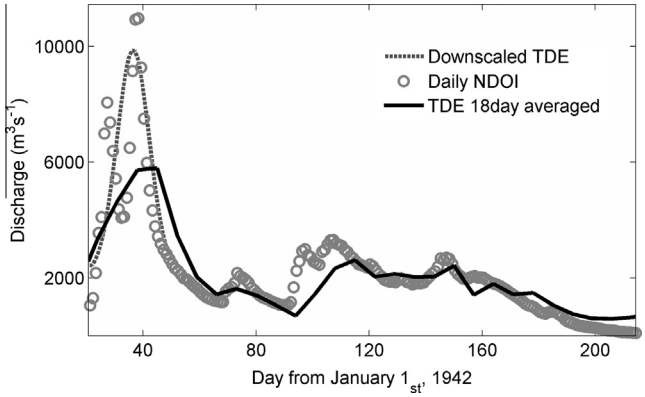

Fig. 4. Original TDE (solid line) and adjusted temporally downscaled TDE (dotted line) vs NDOI estimate (circles).

$$NDOI_{1d} = 1.97 \times TDE_{18d} + 3600; \quad R^2 = 0.71, \tag{4}$$

where $NDOI_{1d}$ and TDE_{18d} denote daily peak flow and 18-day averaged flow, respectively. This relationship is then applied to the peak flow measured by TDE_{18d} to obtain an estimate of the daily peak flow for events $>3500\ m^3\ s^{-1}$ (Fig. 4). To conserve the volume of flow, we require that the area under hydrograph during high flow periods remains the same for both the 18-day averaged flow estimates and the associated daily estimates. Assuming that a flood wave can be approximated by a log-normal curve, we determine the relationship between an 18d average hydrograph and a daily hydrograph by fitting the 31 high-flow events to the following curves:

$$\begin{cases} TDE_{18d}(\tau) = \frac{TDE_p}{\tau\sigma_{TDE}\sqrt{2\pi}} e^{-\frac{(\ln[\tau]-\mu_{TDE})^2}{2\sigma_{TDE}^2}} \\ NDOI_{1d}(\tau) = \frac{NDOI_p}{\tau\sigma_{NDOI}\sqrt{2\pi}} e^{-\frac{(\ln[\tau]-\mu_{NDOI})^2}{2\sigma_{NDOI}^2}} \end{cases}, \tag{5}$$

where TDE_p, μ_{TDE} and σ_{TDE} denote the peak flow, location parameter and standard deviation of the fitted distribution to the hydrograph of an 18d averaged TDE high flow event and, $NDOI_p$, μ_{NDOI} and σ_{NDOI} denote the peak flow, location parameter and the standard deviation of daily NDOI high flow event. Results show that for similar location parameters, σ_{NDOI} is half σ_{TDE} for these events, on average. Assuming that the water resources management measures did not considerably changed this ratio after 1930, we estimate the daily hydrograph from pre-1930 high flow events (TDE > 3500 $m^3 s^{-1}$; 19 events in total) using:

$$TDE'_{1d}(\tau) = \frac{TDE_{18dp}}{\tau\sigma_{SDE}\sqrt{2\pi}} e^{-\frac{(\ln[\tau]-\mu_{TDE})^2}{2\sigma^2_{SDE}}}, \quad (6)$$

where TDE'_{1d} is the adjusted daily TDE, μ_{TDE} is the location parameter of the fitted log-normal curve to the associated TDE high flow event, TDE_{18dp} is the associated 18d averaged peak TDE, and $\sigma_{SDE} = 0.5 \times \sigma_{TDE}$. Fig. 4 tests the applicability of the model for resampling TDE data for a flood event in 1942, and shows that adjusted, downscaled TDE values (e.g. TDE'_{1d}) using Eq. (6) match daily NDOI well.

We next estimate daily Composite Discharge Estimate (CDE) during periods of missing WL data by adjusting TDE estimates using the procedure described in Eq. (6). For other periods the tide-gauge based estimate (TDE) provides a bias check against Sacramento Discharge Estimate (SDE), which may become inaccurate when levee failures occur. In particular, we replace SDE with TDE'_{1d} estimates for peak flows during three periods of major levee failure. These include (a) the extremely high flow events in December 1861 and January 1862; (b) the floods of 1878, 1880 and 1881, which resulted in the construction of the First Comprehensive Flood Control Plan of Sacramento Valley; and (c) the destructive floods in 1907 and 1909, which resulted in authorization of the Sacramento Flood Control System by the Congress in 1917 (James and Singer, 2008).

We also develop and calibrate a model of flow standard deviation σ to provide 95% confidence intervals (CI) for the estimated daily flows (Fig. 5). There is a correlation between the mean of NDOI (estimated via TDE) and σ within an 18-day calculating window, which increases non-linearly with NDOI.

2.2.4. Sediment-discharge rating curve parameters

Ganju et al. (2008) employed hydrologic proxies (monthly unimpaired flows and rainfall records) to downscale the Gilbert (1917) decadal sediment load estimates. They then used the results of Porterfield (1980) to develop a daily estimated sediment load from a rating curve of the form:

$$Q_s = aQ_p^{b+1}, \quad (7)$$

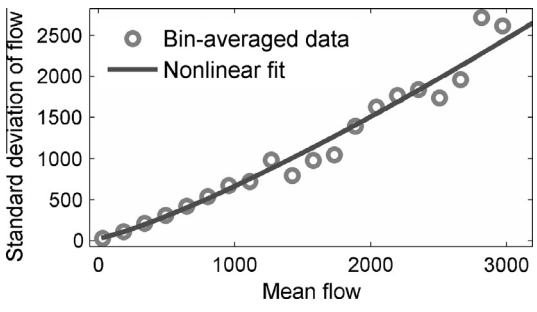

Fig. 5. The relationship between mean and standard deviation within an 18-day calculating window.

to relate daily discharge (Q_p) and daily sediment load (Q_s). In Eq. (7) the parameter a represents the sediment supply and b relates to the erosive power of the stream (Muller and Forstner, 1968; Syvitski et al., 2000; Ganju et al., 2008).

Ogden Beeman and Associates (1992) set parameter $b = 0.1$ for the Sacramento and San Joaquin Rivers for 1955–1990; but their estimate is based on an annual sediment rating curve. Ganju et al. (2008) suggested $b = 0.13$, based on analysis of daily data from WY2000–2003. However, this was a relatively low flow period after the step-change in sediment concentrations in 1999 (Schoellhamer, 2011), and we find that this value of b underestimates sediment load during historical high flow events (e.g. WY1965).

In this study we use Composite Discharge Estimate (CDE) and Eq. (7) to estimate sediment load, based on constraints provided by improved estimates of net deposition (Schoellhamer, 2011). Schoellhamer (2011) estimated net sediment deposition within the SF Bay system during the periods 1861–1892, 1892–1925, 1925–1949, and 1949–1984 from the data of Cappiella et al. (1999), Foxgrover et al. (2004), Fregoso et al. (2008), and Jaffe et al. (1998). These values were 259 Mm^3, −2 Mm^3, 161 Mm^3, and −193 Mm^3, respectively; a negative result represents net erosion. We employ an iterative approach and take the steps outlined below to calibrate the rating curve parameters a and b for three time periods.

2.2.4.1. Step I – Estimating rating curve parameter b. To estimate b, we re-analyze the sediment load from the Sacramento and San Joaquin rivers (described in Section 2.1.3). The observed data are divided into three time periods (Fig. 6). The first period extends from the beginning of sediment load observations (1956) to 1968, the year that Oroville dam (Fig. 1) was completed, subsequently trapping large volumes of sediment and markedly altering sediment transport during large floods below both Oroville Dam and in the Delta (James, 2006, 2010). The second period extends from 1969 to 1998, the time between the completion of Oroville Dam and a step decrease in SSC (Schoellhamer, 2011). The third period, from 1999 to 2011, represents the time in which the sediment supply in delta tributaries is depleted and the system is largely supply limited (Schoellhamer, 2011). To prevent the fitted curve being biased by low flow periods, the NDOI and sediment load values were bin-averaged to 50 evenly spaced bins in term of NDOI values. Fig. 6 shows the relationship between bin-averaged discharge and sediment load, and Table 1 represents the results of sediment rating curve regression analysis for parameter b. As a first estimate, we assume that b is the same for 1862–1955 and 1956–1968, because the system was transport capacity limited during both periods (Schoellhamer, 2011). Below, we iteratively re-adjust b for 1862–1955, over each time span for which Schoellhamer (2011) estimated net sediment deposition. Note that fitting a single curve to the whole range of flow regimes underestimates the sediment load during low flows (Fig. 6), during which, however, only ~10% of the annual load is transported. This error is therefore negligible. Note that a split rating curve approach, in which separate sediment flux curves are fit to high and low flow portions of the flow regime, produces an under-constrained problem with more unknowns than knowns in the mass balance equation used to iterative revise of a and b (see below).

2.2.4.2. Step II – Estimating rating curve parameter a. We assume that parameter a is constant within each time span. Thus, using the estimate of b from step I, we constrain a by requiring that the net sediment transport ($I_j - O_j$) be equal to the total deposited sediment over a time period (ΔS_j):

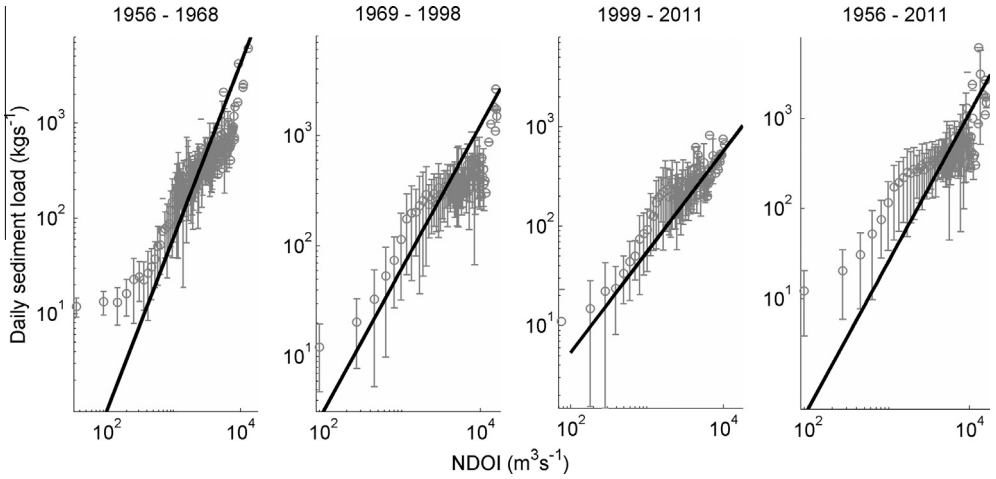

Fig. 6. Sediment transport rating curve; bin-averaged NDOI vs sediment load from Sacramento and San Joaquin rivers plotted in log–log space.

Table 1
Rating curve parameter b ($Q_s = aQ_p^{b+1}$).

Parameters	1956–1968	1969–1998	1999–2011	1956–2011
b	0.827	0.297	0.012	0.644

$$\Delta S_j = I_j - O_j = \int_{t=t_1}^{t=t_2} Q_{si}dt - O_j \approx \int_{t=t_1}^{t=t_2} a_j Q_i^{b_j+1}dt - O_j; \quad j = 1,2,3,4, \tag{8}$$

where Q_i and Q_{si} denote daily discharge and sediment load for day i (where $t_1 \leqslant t \leqslant t_2$), respectively, a_j and b_j are rating curve parameters for time period j that lasts from time t_1 to time t_2, ΔS_j denotes the net deposition or erosion within the system for each time span defined by Schoellhamer (2011), and j = 1–4 represents the periods 1861–1892, 1892–1925, 1925–1949, and 1949–1984.

The sediment output (O_j) includes (i) export to the Ocean through the Bay and (ii) permanently removed materials from the SF Bay system (e.g. through dredging, aggregate mining, and borrow pit mining); thus:

$$O_j = O_{export} + O_{removed}. \tag{9}$$

We do not discriminate the different particle sizes in total load estimates. However, most suspended sediment is fine flocculated cohesive sediment (Manning and Schoellhamer, 2013) and most removed sediment is sand (Dallas and Barnard, 2011).

Due to difficulties inherent in measuring flow and sediment discharge in the deep, wide, and energetic Golden Gate, there are only a handful of measurements defining SF Bay sediment export to the Pacific Ocean for which the median suspended particle (including flocs) size was about 40 microns (Erikson et al., 2013). Schoellhamer (2011) argues that $O_{export} = Sc_o$ in well-mixed estuarine waters, where S = suspended sediment mass S and c_o = outflow coefficient (with units of time^{-1}). Before ~1998, S is assumed to be equal to its maximum value (S_{max}) due to transport regulation of suspended sediment; thus $O_{export} = S_{max}c_o$. Schoellhamer (2011) thus estimates an average sediment outflow of 8.4 Mt yr^{-1} for SF Bay for 1860–1999, which we use in Eq. (9).

Dallas and Barnard (2011) compiled historical records and estimated that since 1900, at least 200 Mm^3 of sediment has been permanently removed ($O_{removed}$) from SF Bay via dredging and borrow pit mining (mainly sand). Specifically, about 64 Mm^3 and 90 Mm^3 of sediment were permanently removed during the periods 1900–1949, and 1949–1984, which we use in Eq. (9). However, these exclude pre-1900 removal and may not be complete for the period after 1900. Additional historic records show that ~1.85 Mm^3 and ~2.35 Mm^3 was permanently dredged from Rincon Rock, SF Harbor and Oakland Harbor, SF Bay between 1873–1889, and 1890–1899, respectively (US Army Corps of Engineers, 1915). We use these values in Eq. (9) for pre-1900 estimates. An unknown amount of mining sediment was deposited on floodplains pre-1910 (e.g. due to levee failures), and was not considered in either the bathymetric surveys or in removed material. We are unable to correct for this loss due to lack of information.

To find the optimal rating curve parameter a for each period, we test a range of values of a from 0 to 1 with the step size of 10^{-8}. We then calculate daily sediment transport (Q_{si}), and compare the integral estimated input ($I_j = \int_{t=t_1}^{t=t_2} Q_{si}dt$) with the sum of storage and output ($\Delta S_j + O_j$). Choosing the value of a that provides the best estimate (i.e. results in the least square difference between I_j and $\Delta S_j + O_j$, as the best estimates of a_j.

Schoellhamer (2011) calculates the change in bed volume using bathymetric data before 1984. Rating curves fitted to daily values (Fig. 6b and c) suggest that a should be about 3.23×10^{-3} and 0.045 for the periods 1985–1998, and 1999–2011, respectively. As these values represent only the load from the Central Valley, we multiply them by 1/0.4 (McKee et al., 2013) to reflect the contribution of local tributaries in total load delivered to SF Bay from 1984 to 2011.

2.2.4.3. Step III – Smoothing the variation of parameter a between periods. Step II provides estimates of a that make step changes from one period to the next, which may cause unrealistic sharp changes in sediment supply. Only under specific circumstances (e.g. beginning of hydraulic mining activities in the late 1850s, and depletion of sediment pool in the late 1990s) would sediment supply change drastically this way. Also, the bathymetric observations that Schoellhamer (2011) used for calculation of net sediment deposition were made over periods of ~10 years (Cappiella et al., 1999; Fregoso et al., 2008; Foxgrover et al., 2004; Jaffe et al., 1998). To avoid sharp changes in parameter a between bathymetric survey periods we assume that parameter a changes over a decade between each period. For example, the parameter a estimated for 1892–1925 was constrained to linearly decrease between 1920 and 1930 to reach the value estimated for 1925–1949.

2.2.4.4. Step IV: Re-adjusting parameter b. The smoothing process for a (described in Step III) causes the estimated sediment delivery for each time span to change. To conserve the mass in the system,

Table 2
Rating curve parameters ($Q_{si} = aQ_i^{b+1}$).

Parameters	1849–1861	1862–1892	1893–1925	1926–1949	1950–1968	1969–1984	1985–1998	1999–2011
a	0.281	1.91×10^{-8}	5.10×10^{-8}	8.18×10^{-8}	4.08×10^{-6}		0.020	0.281
b	0.012	2.019	1.931	1.951	1.392	1.289	0.297	0.012
Mass balance relative error	–	0.084	0.135	0.077	0.053		–	–
Estimated mass balance error (Mt)	–	38.55	43.47	26.36	12.81		–	–

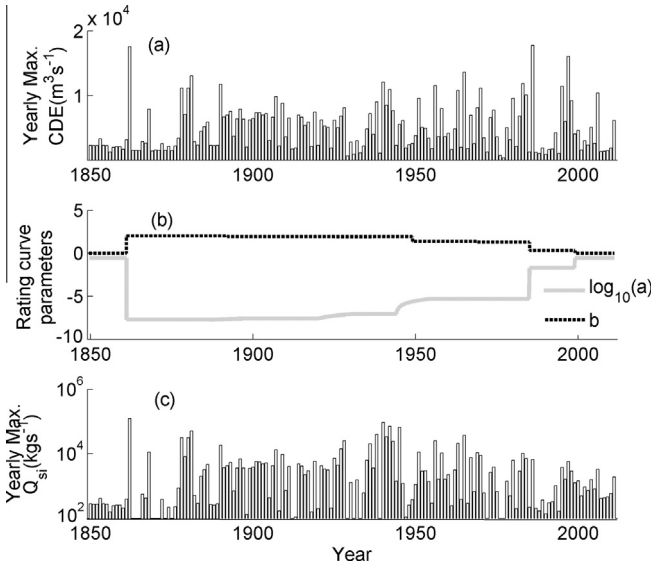

Fig. 7. Estimated yearly maximum discharge (Panel a), rating curve parameters (Panel b) and sediment load (Panel c) to SF Bay (1849–2011).

we re-adjusted b_j such that I_j and $\Delta S_j + O_j$ are equal again. This estimated parameter *b* was then compared to the previously estimated *b*. If the difference was >10% a further iteration through steps II to IV was made, until the difference between estimated parameter *b* for two following trials was less than 10%. Table 2 shows the final estimates for rating curve parameters from 1849 to 2011 that have been used in this study. Fig. 7a–c represent the estimated yearly maximum daily discharge, variation in rating curve parameters *a* and *b*, and the estimated yearly maximum daily sediment load to SF Bay, respectively. Table S1 represents the annual averaged values for these parameters (see Supplementary material).

3. Results

3.1. Discharge Estimation (CDE)

To confirm its applicability for discharge estimation, SDE (provided as a Supplementary material) is first compared to NDOI data for 1930 to 1944, and is then validated using both NDOI for 1945–1946 and the 18d averaged TDE 1881–1929 (Moftakhari et al., 2013). Then, pre-1930 CDE (SDE and TDE combined, Sections 2.2.2 and 2.2.3) is validated using four series of data (a) ERI 1906–1944, (b) observed discharge at Red Bluff, CA 1891–1944, (c) total monthly precipitation 1851–1944, and (d) SRI 1879–1884 (see Section 2.1.4 for more information). For cases in which we compare the estimated/observed values of a parameter from two different sources/approaches, we use the Nash–Sutcliffe efficiency coefficient, an indicator of fit that is widely used to assess the predictive power of hydrologic models. For comparisons between different variables (e.g. discharge and rainfall) we use a correlation coefficient to assess the reliability.

Comparison to NDOI: Comparison of SDE with NDOI data for 1930 to 1944, the calibration time period yields a Nash–Sutcliffe efficiency coefficient of 0.89 (Fig. 8a). Over the 1945–1946 validation period, the Nash–Sutcliffe efficiency coefficient is 0.92 (Fig. 8b).

Comparison to TDE: Monthly averaged flow (TDE) estimates from Moftakhari et al. (2013) from 1881 to 1929 are compared against monthly averaged SDE in Fig. 9a. The correlation coefficient for this period is 0.84.

Comparison to the Eight-River Index (ERI): To assess the robustness of CDE we compare it to measures of unimpaired SF Bay inflow. Fig. 9b shows the monthly-average of CDE versus ERI (December–May) for the periods 1906–1944. The correlation coefficient is 0.82, and a linear regression yields $Y = 0.648X + 465.42$ with an R^2 of 0.67.

Comparison to flow at Red Bluff, CA: To compare Red Bluff flows with CDE, and reduce the effect of time-lags we plot weekly-averaged Red Bluff flows against weekly-averaged CDE over the period 1891–1944 (Fig. 9c). The correlation coefficient is 0.88, and a linear regression yields $Y = 0.252X - 90.39$ with an R^2 of 0.77. Approximately 25% of the flow from the entire basin enters the river above Red Bluff, even though the gauge at Red Bluff drains ~14% of the total watershed.

Comparison with precipitation data: Fig. 9d shows annual total precipitation at Sacramento, CA versus CDE, 1849–1944. In this case, the correlation coefficient is 0.82, and a linear regression yields $Y = 0.057X + 37.79$ with an R^2 of 0.67. Thus, years with high rainfall at Sacramento produce correspondingly large annual flows, despite soil storage effects and basin-wide variability in precipitation.

Comparison with SRI: The SRI provides a valuable historical check on flow estimates during the peak of hydraulic mining activities 1879–1884. Though similar to a monthly averaged NDOI it does not consider exports and precipitation. Fig. 10 compares monthly-averaged CDE (with errorbars) to SRI 1879–1884; the Nash–Sutcliffe efficiency coefficient for this period is 0.78. The downscaled TDE is plotted as well to show the compatibility of these flow estimates.

To summarize these comparisons, CDE is closely comparable to diverse hydrologic measures for SF Bay and the Sacramento River over the last 160 years, as verified by good correlation coefficients and Nash–Sutcliffe values. Therefore, the CDE approach provides a reliable method for hindcasting historic daily flows.

3.2. Sediment transport estimates

The CDE data validated in Section 3.1 are next used to estimate daily sediment flux into SF Bay from WY1850 to 2011 (see Section 2.2.4 for methods). Fig. 11 shows the yearly-average estimated load from 1956 to 2011 using NDOI and the integral sediment constraints vs. the average annual load estimated from observed data described in Section 2.2.3. The results suggest that the contribution of the Central Valley to the delivered load SF Bay is different during high-load WYs (averaging >10,000 ton/day) and low-load WYs (<10,000 ton/day). During low-load periods the correlation coefficient is 0.80, and a linear regression yields $Y = 0.50X + 3000$ with an R^2 of 0.84. The estimated slope therefore

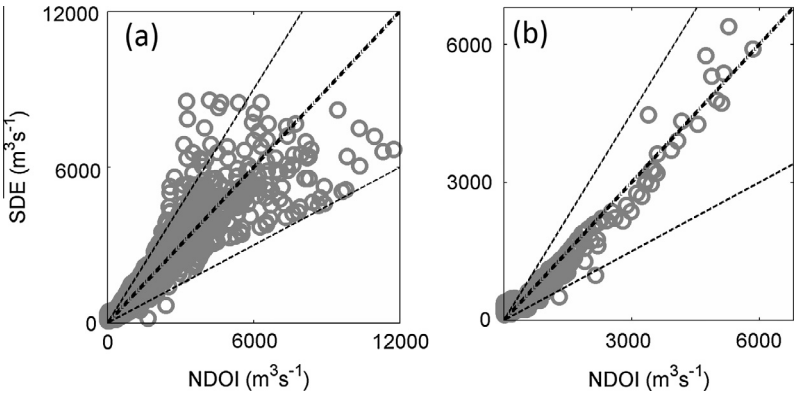

Fig. 8. Panel (a): checks the applicability of SDE; Panel (b) compares daily SDE for WY1945–1946 to NDOI to validate the model. Circles show the daily values, dash-dot line shows the equal line and dashed lines show the estimated 95% confidence interval.

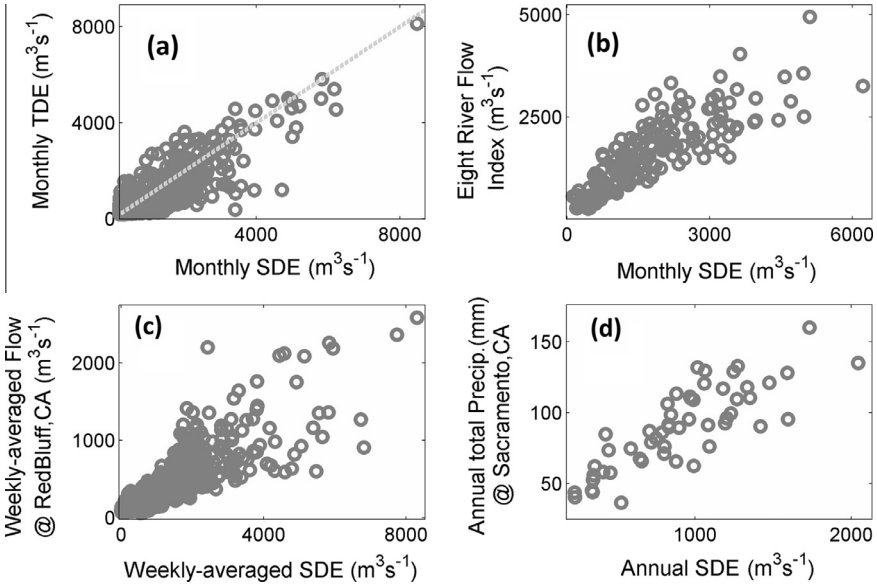

Fig. 9. Validation of CDE via comparison to four hydrologic measures; panel (a): vs TDE; panel (b): vs ERI; panel (c): vs discharge observed at Red Bluff, CA; panel (d): vs annual total precipitation.

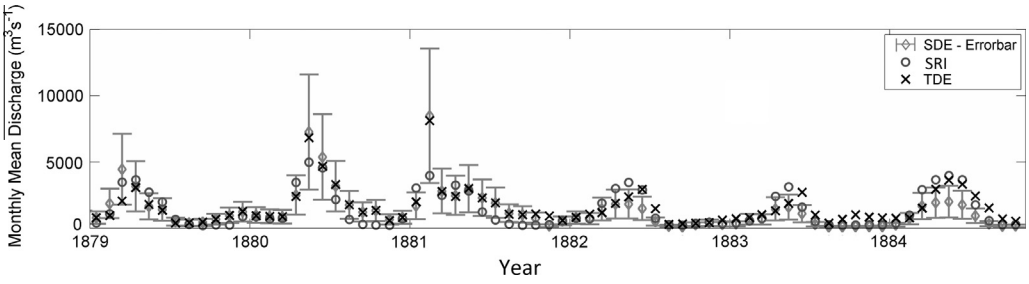

Fig. 10. Monthly-averaged CDE vs monthly mean discharge (aka Six-River index) from the Central Valley and adjusted downscaled TDE.

suggests that ~50% of the load delivered to the Bay during low-load conditions comes from the Central Valley and the rest from local tributaries. By contrast, the transport capacity limitation of sediment delivery from the Central Valley causes this percentage to change over high-load periods. Since 1956, our results suggest that local tributaries contribute ~85% of sediment delivered to SF Bay during high-load years, compared with ~50% during low-load years.

Fig. 12a shows CDE estimates for WY1850 to WY1929, and Fig. 12b shows the estimated daily sediment flux to SF Bay from WY1850 to WY2011. Also, Fig. 7a and c shows the yearly maximum discharge and yearly maximum sediment flux to SF Bay between 1849 and 2011, respectively. These results suggest that the largest daily sediment flux (125,000 kg s^{-1}) since 1849 occurred in January 1862 (Fig. 7c), due to the second largest daily peak flow (CDE estimate of 17,600 m^3 s^{-1}) and the largest 18-day averaged peak flow in the last 160 yrs (Moftakhari et al., 2013). However, a significant uncertainty must be ascribed to the 1862 discharge level, because the amount of floodplain inundated was

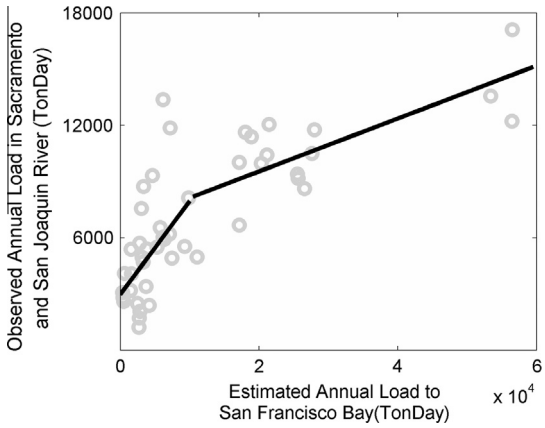

Fig. 11. Estimated annual load vs annual SSC load observed at Sacramento, CA (1956–2011).

much larger than any subsequent flood. Thus, the flood discharge may have been significantly larger than our estimate and large amounts of sediment may also have been deposited throughout the Central Valley and Delta region. Regardless, the largest measured daily peak flow that occurred in 1986 (17,900 $m^3 s^{-1}$) is slightly larger than our estimated daily peak flow for 1862.

Although several large floods occurred between 1849 and 1853, the system was more supply limited (compared to the late 19th century) and no large sediment flux peak is evident. Large peak flows in WYs 1878, 1879, 1880, 1881, 1890 coincided with the huge amount of sediment that was released to the watershed due to hydraulic mining, producing very large annual sediment fluxes in the late 19th century. Though hydraulic mining was banned in 1884, the sediment supplied by previous mining activities continued to move downstream during high flow events. Land development, timber harvest and agricultural activities along with delayed debris from hydraulic mining activities produced large daily sediment loads during floods in WYs 1927, 1928, 1938, 1940, 1941, 1942, and 1945. None of these events supplied as much sediment as the 1862 flood, however.

4. Discussion

Since 1998, San Francisco Bay has become significantly less turbid (Schoellhamer, 2011) and is facing the prospect that contaminated mercury sediments may begin to erode if annual sediment export (through the Golden Gate or from sand mining and dredging) is more than sediment inputs (see Bouse et al., 2010). Our evaluation of sediment export over time suggests that the parameters *a* (sediment supply) and *b* (stream power) and the river flow have significantly changed over time (Fig. 7b), and that these changes reflect the diminished annual supply of sediment to the Bay. A related change, with possible implications for nutrient transport and the biogeochemical cycle in the bay and coastal ocean, is that significant snow-melt driven freshets and spring season sediment pulses have decreased. Decadal cycles in river flow and sediment flux are also evident in the data; e.g., relatively low flows from 1912 to 1937 were followed by large flows from 1938 to 1945.

Overall, our estimates of daily sediment fluxes using an integral constraint suggest that the total sediment load delivered to SF Bay because of hydraulic mining and land development activities was considerably larger than previous estimates, especially during the second half of the 20th century (Fig. 13). The area of reclaimed land in the Bay Area almost doubled by the late 1920s (~1700 km^2), relative to the beginning of the 20th century (~950 km^2) (Thompson, 1957); loss of access to both floodplain and intertidal areas reduced the area over which sediment can deposit, possibly focusing sediment deposition during the mid-20th century in the remaining wetted areas and inflating the observed deposition. We speculate that the elevated mid-century sediment load, while possibly augmented by the effects of urbanization and agricultural activities, may also reflect the residual effects of hydraulic mining and other land-management practices such as logging. Folsom Dam on the American River only began holding water and capturing sediment in 1956, and Oroville dam on the Feather River was

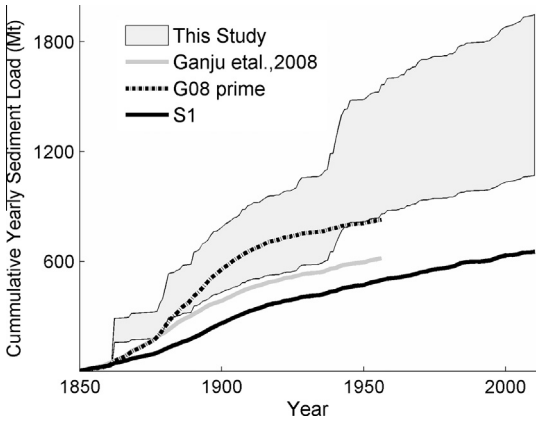

Fig. 13. Comparison of our cumulative sediment load estimate (aka reality scenario) with the previous studies and load under the assumption that rating curve parameters remain the same as pre-Gold rush values (Scenario S1); bulk density of 850 kg m^{-3} (Porterfield, 1980; Jaffe et al., 2007); G08 shows the results of Ganju et al. (2008) divided by 0.9; G08_prime is the result of applying suggested rating curve by G08 to SDE divided by 0.9.

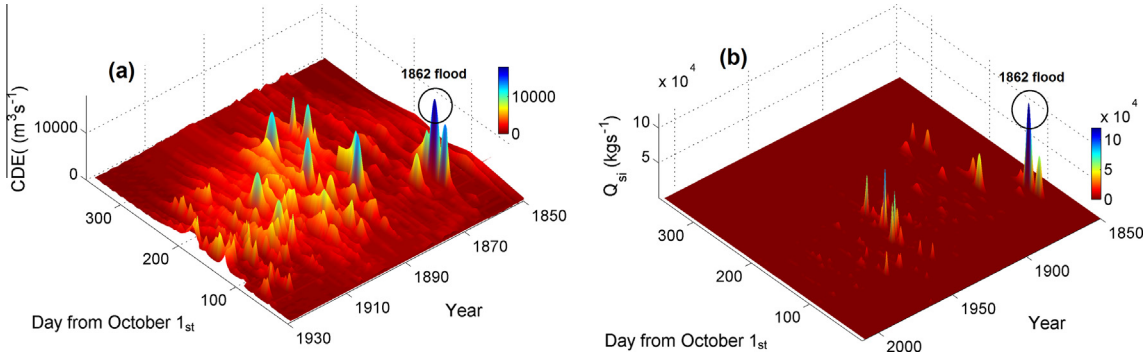

Fig. 12. Panel (a): CDE (1849–1929); Panel (b): daily sediment transport to SF Bay (1849–2011).

only finished in 1968. In fact, large sediment concentrations on the Feather River during the floods in 1950s and early 1960s were attributed to the residual effects of hydraulic mining (James, 2004). It is also possible that greatly increased logging and clear-cutting between about 1940 and 1970 (Burns, 1972; Laudenslayer and Darr, 1990) increased sediment fluxes during the mid-20th century. While further research is needed to determine the cause of the mid-century pulse, it seems clear that it was augmented by significant river flow events, compared to the relatively low flow from 1912 to 1937. At the close of the 20th century, depletion of the sediment pool reduced the largest daily peak flows in 1986 and 1997 to only 7000 kg s^{-1} and 6000 kg s^{-1}, respectively, which are small values considering the magnitude of flooding (Fig. 7c; see also Schoellhamer, 2011).

Fig. 13 compares our cumulative sediment load estimate from 1849 to 2011 with those estimated by Ganju et al. (2008) (G08). They have estimated sediment load from the Central Valley (1851–1958), while we have estimated total sediment load from both the Central Valley and local tributaries adjacent to the Bay. To compare our results with their estimates we have divided their estimates by 0.9 to reflect the pre-1955 contribution of local tributaries to total load (Ogden Beeman and Associates, 1992). This comparison quantifies the effect of employing different approaches of estimating river flow and the parameters a and b in Eq. (7). The estimated sediment load from our model is greater than G08 for four main reasons. First, the approach that we have employed and the proxies that we have used to estimate historic daily flows are different, which affects the estimation of sediment load. To demonstrate this difference, we applied G08's sediment rating curve to our CDE data (G08-prime in Fig. 13). The cumulative load estimates by G08-prime for 1849–1955 are 30% larger than G08, indicating that the effect of using different discharge estimates is considerable. Second, inclusion of sediment pulse in the mid-20th century produces a large difference in mass balance and affects the supply parameter a, and thus the sediment load estimates. A third difference between G08 and our estimate is how the rating curve parameters a and b vary over time. In G08 parameter a gradually increased and decreased, before and after 1890, respectively, because they did not consider the second pulse of sediment in the 20th century. We assumed rating curve parameter a to be constant during each time span and to linearly vary between the time spans. Finally, G08 assumed that the stream power parameter b is constant over time, while we allowed b to vary between time periods (Table 2).

To determine the contribution of natural processes and human activities to the time history of sediment load, we next analyze one more scenario. Scenario S1 (Fig. 13) shows the cumulative sediment load that would have occurred under pre-hydraulic mining sediment supply and stream-power conditions, given the measured flow. Sediment supply (parameter a) and stream power (parameter b) are kept at the pre-hydraulic mining values between 1862 and 2011. S1 produces a cumulative load of ~650 Mt, ~45% (35–60%) of the estimated ~1500 ± 400 Mt (uncertainty explained below) which we estimate to have been supplied during this period. Hence, ~55% (45–75%) of the cumulative sediment load since 1849 is directly attributable to anthropogenic alteration of the sediment supply.

The timing and magnitude of the annual peak flow has changed considerably over time, likely due to flood control projects, diversion for irrigation and human consumption, and climate change (Knowles, 2002; Moftakhari et al., 2013). We evaluate the effect of long-term changes in the annual hydrograph on sediment load to the Bay in Fig. 14. Fig. 14a compares CDE-based hydrographs for historic flows (averaged over 1849–1945, by year-day), and the modern flow regime (1946–2011). Both the timing of the annual peak flow and the total volume of water changed considerably in the modern, managed era compared with the much less impaired flow regime of the late 19th century and the early 20th century. Snowmelt-driven spring freshets produced the annual peak flows in many years prior to 1940s. Diversions have reduced the total volume of water delivered to SF Bay in the modern system by ~35% compared with the pre-1946 system (~3.9 km^3/yr versus ~2.4 km^3/yr total inflow in modern system). This 35% reduction is compatible with the ~30% reduction suggested by Moftakhari et al. (2013), despite the different time periods evaluated (WY1850–1945 here vs. WY1858–1900). The relative stationarity in flow statistics pre-1945 suggests that the majority of flow regime changes have been produced by anthropogenic and climate impacts which occurred over the past 70 years.

Fig. 14b compares sediment load hindcasts averaged by year-day for historic (1849–1945), and the modern (1946–2011) flow regime. The results suggest that the timing of peak sediment loading has changed over time. Storms and snow-melt driven discharge, which produced peaks from February to May in the historic system, have now been shifted to an earlier year date, and are mostly associated with winter storm events. An approximately 35% reduction of annual flow since the 19th century along with decreased sediment supply has produced an average sediment load in the modern system (~5.9 Mt/yr) that is only ~50% of the 19th and the early 20th century load (~11.7 Mt/yr).

Strong seasonality in the flow regime in SF Bay causes the majority of sediment load to be transported during high flow events. Specifically, Fig. 15 shows that on average 40%, 75%, and 90% of the total load moves during top 1%, 10%, and 50% flow days, respectively. Thus on average, 90% of the yearly load moves during the wet half of the year, while only 10% moves during the dry season. The results also suggest a shift in seasonality over time. While ~45% of the total load was delivered during top 1% flow days 1850–1945, only ~25% is currently transported during the top percentile. Fig. 14b supports the results of Fig. 15, and suggests that

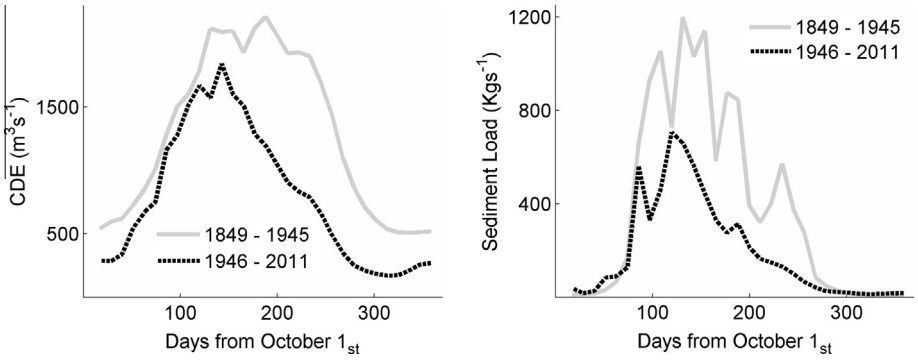

Fig. 14. Panel (a): CDE by year-day, averaged over 1849–1945, and 1946–2011; Panel (b): Sediment load estimates by year-day, averaged over the same periods.

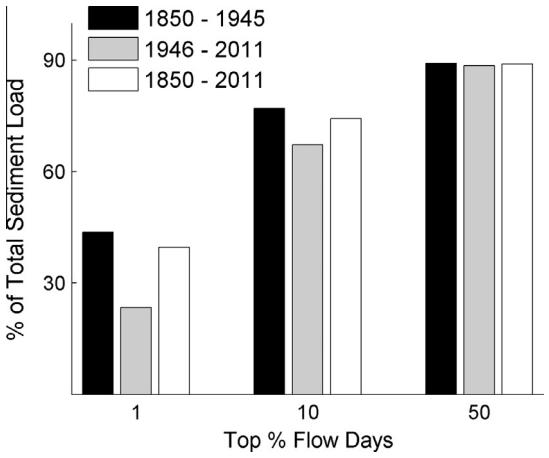

Fig. 15. Contribution of high flow days in total sediment load.

the seasonality of sediment flux has shifted over time because spring-melt floods have decreased. Hence, most sediment input now occurs in winter (this assumes that parameters a and b do not change seasonally, which we cannot evaluate). While historically ~70% of the total annual load was delivered in Winter (Dec. to March), and ~25% was delivered in Spring (Apr. to June), ~80% of the load is delivered during winter storm-driven flows in the modern system and less than 15% in spring.

Evaluating the significance of our sediment load estimate requires understanding the magnitude of likely errors, which may be systematic (due to bias) or random. The mean of random errors such as bathymetric measurement errors and digitization errors are assumed to be close to zero when averaged spatially. Thus, systematic errors are likely to be the most important limitation to the accuracy of our results. One possible source of error is incorrect vertical datum correction between surveys of the same subembayment (Fregoso et al., 2008). This type of systematic error is expected to be less than 0.1 m, and in the worst case may cause an error of up to 120 Mm^3 (~100 Mt) in estimates of bay volume change between surveys, when integrated over SF Bay (Schoellhamer, 2011). Four surveys were used in this work so this error applies to each of the three resulting volume change calculations.

Another likely issue is that spatial variability in bed elevation due to tectonic deformation and earthquakes was not considered by Schoellhamer (2011). Spatially varying vertical land motion contributes to different observed rates of sea level rise. Sea level rise at three water level gauges with long (greater than 40 years) and complete records is 2.01 ± 0.21 mm yr^{-1} at San Francisco, 0.82 ± 0.51 mm yr^{-1} at Alameda, and 2.08 ± 2.74 mm yr^{-1} at Port Chicago (Zervas, 2009). The long-term tectonics occur in only one direction and this type of uncertainty ideally should be treated as a bias in total load. Here, however, we treat the error associated with this deformation as a random error because deformation direction and rates vary spatially, deformation adjacent to San Pablo and Suisun Bays is unknown, and subtidal deformation is unknown (Burgmann et al., 2006). In addition, tectonic plates in the region were perturbed by large earthquakes in 1868, and 1989 and, in particular, 1906 (Jaume and Sykes, 1996). However, within the SF Bay region "there occurred no general change of elevation of sufficient magnitude to be detected with certainty" due to 1906 earthquake (Lawson et al., 1908), the bench-mark surveys suggest relative vertical land motions of up to 0.035 m between San Francisco (Presidio) and Sausalito (Zervas, 2009). An order of magnitude estimate of sediment volume error attributed to long-term tectonics over the last 150 yrs is 0.15 m ($1\ mm\ yr^{-1} \times 150\ yr = 0.15\ m$). An upper estimate of relative deformation due to three large earthquakes is 0.1 m (3 earthquakes × 0.035–0.1 m). These factors create potential errors of up to 180 Mm^3 (~150 Mt) and 120 Mm^3 (~100 Mt), respectively.

Another possible source of error occurs in the difference between estimated input (I_j) and the sum of storage and output ($\Delta S_j + O_j$) in Eq. (8). From Table 2 the total (e.g. cumulative) mass balance error associated with our sediment load estimates is approximately ±120 Mt. As discussed earlier, the estimated error due to uncertainty in flow is ±260 Mt, and the maximum total error associated with our estimates would be the square root of the sum of the squares (e.g. $\sqrt{3 \times 100^2 + 100^2 + 150^2 + 120^2 + 260^2} \approx 400$ Mt). Our results therefore suggest that 1500 ± 400 Mt of sediment was released into the SF Bay system over the last 160 yrs. However, other factors contributing to the error, such as estimated sediment export to the ocean cannot easily be evaluated. We also note that bathymetric surveys do not fully survey intertidal areas and ignore flood plains, and thus may have under-estimated total sedimentation. On the other hand, large areas of the bay, including both floodplains and tidal flats were removed from the system by 1900, so that they would not have received sediment, except during dike breaching events. It is not possible to estimate errors in the sediment load estimates associated with sedimentation in areas not surveyed.

5. Conclusions

This study provides improved estimates of daily inflow and sediment delivery to SF Bay, using approximately 80 years of daily water stage data for Sacramento, CA from as early as WY1850. After correcting for changes to channel depth and water level variance, water level based discharge estimates are combined with NDOI and TDE flow estimates to provide a composite delta inflow record back to WY1850. Our estimates suggest that natural processes combined with hydraulic mining and agricultural activities released ~1500 ± 400 Mt of sediment to SF Bay from 1849 to 2011. The average annual volume of delivered sediment is ~50% lower in the modern system than during the peak hydraulic mining sediment pulse. The results also suggest that since 1956, local tributaries contribute ~85% of sediment delivered to SF Bay during high flow years, compared with ~50% during low flow years. We estimate that ~55% (45–75%) of the sediment delivered to the estuary between 1849 and 2011 was the result of anthropogenic alteration in the watershed that increased sediment supply. The large increases in sediment input due to hydraulic mining, urbanization, logging, and other anthropogenic developments emphasize how far the system has departed from its pre-hydraulic mining conditions prior to 1862.

Acknowledgments

Support for this project was provided in part by a Miller Foundation grant to the Institute of Sustainability and Systems at Portland State University and a Portland State Research enhancement grant. D.A. Jay and S.A. Talke were supported in part by the National Science Foundation grant: Secular Changes in Pacific Tides, OCE-0929055. S.A. Talke was supported in part by National Science Foundation grant: 19th Century US West Coast Sea Level and Tidal Properties, OCE-1155610, and the US Army Corps of Engineers, award number W1927N-14-2-0015. D.H. Schoellhamer was supported by the Delta Science Program and USGS Priority Ecosystem Science Program and this article is contribution number 52 from the USGS CASCaDE project (Computational Assessments of Scenarios of Change for the Delta Ecosystem). Scott A. Wright and

Mathieu Marineau at USGS California Water Science Center in Sacramento, CA are acknowledged for contributing to the digitization of data, and Neil Ganju (USGS, Woods Hole, MA) is acknowledged for providing data and helpful discussion. L.M. Hunsaker is acknowledged for providing the Thomas Logan Hydrographs used in this study. Mick Van der Wegen and two other anonymous reviewers are acknowledged for sharing their valuable thoughts which have substantially improved the manuscript.

Appendix A. Supplementary material

Supplementary data associated with this article can be found, in the online version, at http://dx.doi.org/10.1016/j.jhydrol.2015.08.043.

References

Allen, G.P., Salomon, J.C., Bassoullet, P., Du Penhoat, Y., De Grandpre, C., 1980. Effects of tides on mixing and suspended sediment transport in macrotidal estuaries. Sediment. Geol. 26, 69–90.

Barnard, P.L., Schoellhamer, D.H., Jaffe, B.E., McKee, L.J., 2013. Sediment transport in the San Francisco Bay coastal system: an overview. Mar. Geol. 345, 3–17. http://dx.doi.org/10.1016/j.margeo.2013.04.005.

Booker, M.M., 2013. Down by the Bay: San Francisco's History between the Tides. University of California Press, Berkeley, California.

Bouse, R.M., Fuller, C.C., Luoma, S.N., Hornberger, M.I., Jaffe, B.E., Smith, R.E., 2010. Mercury-contaminated hydraulic mining debris in San Francisco Bay. San Francisco Estuary Watershed Sci. 8 (1), jmie_sfews_11015.

Burgmann, R., Hilley, G., Ferretti, A., Novali, F., 2006. Resolving vertical tectonics in the San Francisco Bay Area from permanent scatter InSAR and GPS analysis. Geology 34 (3), 221–224.

Burns, J.W., 1972. Some effects of logging and associated road construction on Northern California streams. Trans. Am. Fish. Soc. 101 (1). http://dx.doi.org/10.1577/1548-8659(1972)101<1:SEOLAA>2.0.CO;2.

Cai, H., Savenije, H.H.G., Jiang, C., 2014. Analytical approach for predicting fresh water discharge in an estuary based on tidal water level observations. Hydrol. Earth Syst. Sci. Discuss. 11, 7053–7087. http://dx.doi.org/10.5194/hessd-11-7053-2014.

Cappiella, K., Malzone, C., Smith, R., Jaffe, B., 1999. Sedimentation and Bathymetry Changes in Suisun Bay (1867–1990). U.S. Geological Survey Open-File Report 99-563.

Chen, S., Zhang, G., Yang, S., Shi, J.Z., 2006. Temporal variations of fine suspended sediment concentration in the Changjiang River estuary and adjacent coastal waters, China. J. Hydrol. 331 (1–2), 137–145. http://dx.doi.org/10.1016/j.jhydrol.2006.05.013.

Cheng, R.T., Gartner, J.F., 1985. Harmonic analysis of tides and tidal currents in south San Francisco Bay, California. Estuar. Coast. Shelf Sci. 21, 57–74.

Chua, V.P., Fringer, O.B., 2011. Sensitivity analysis of three-dimensional salinity simulations in North San Francisco Bay using the unstructured-grid SUNTANS model. Ocean Model. 39, 332–350.

Conner, G., 2005. History of weather observations, Sacramento, California 1849–1948. NOAA's National Climatic Data Center, Asheville, North Carolina, http://mrcc.sws.uiuc.edu/FORTS/histories/CA_Sacramento_Conner.pdf.

Conomos, T.J., Peterson, D.H., 1977. Suspended-particle transport and circulation in San Francisco Bay, an overview. Estuar. Process. 2, 82–97.

Dallas, K.L., Barnard, P.L., 2011. Anthropogenic influences on shoreline and nearshore evolution in the San Francisco Bay coastal system. Estuar. Coast. Shelf Sci. 92, 195–204. http://dx.doi.org/10.1016/j.ecss.2010.12.031.

Erikson, L.H., Wright, S.A., Elias, E., Hanes, D.M., Schoellhamer, D.H., Largier, J., 2013. The use of modeling and suspended sediment concentration measurements for quantifying net suspended sediment transport through a large tidally dominated inlet. Mar. Geol., Special Issue San Francisco Bay 345, 96–112.

Fisher, T.R., Carlson, P.R., Barber, R.T., 1982. Sediment nutrient regeneration in three North Carolina estuaries. Estuar. Coast. Shelf Sci. 14 (1), 101–116. http://dx.doi.org/10.1016/S0302-3524(82)80069-8.

Foxgrover, A.C., Higgins, S.A., Ingraca, M.K., Jaffe, B.E., Smith, R.E., 2004. Deposition, Erosion, and Bathymetric Change in South San Francisco Bay: 1858–1983. U.S. Geological Survey Open-File Report 2004-1192.

Fram, J.P., Martin, M.A., Stacey, M.T., 2007. Dispersive fluxes between the coastal ocean and a semienclosed estuarine basin. J. Phys. Oceanogr. 37, 1645–1660. http://dx.doi.org/10.1175/JPO3078.1.

Fregoso, T.A., Foxgrover, A.C., Jaffe, B.E., 2008. Sediment Deposition, Erosion, and Bathymetric Change in Central San Francisco Bay: 1855–1979. U.S. Geological Survey Open-File Report 2008-1312.

Ganju, N.K., Schoellhamer, D.H., 2009. Calibration of estuarine sediment transport model to sediment fluxes as an intermediate step for simulation of geomorphic evolution. Cont. Shelf Res. 29, 148–158.

Ganju, N.K., Knowles, N., Schoellhamer, D.H., 2008. Temporal downscaling of decadal sediment load estimates to daily interval for use in hindcast simulations. J. Hydrol. 394, 512–523.

Gelfenbaum, G., 1983. Suspended-sediment response to semidiurnal and fortnightly tidal variations in a mesotidal estuary: Columbia River, USA. Mar. Geol. 52 (1–2), 39–57. http://dx.doi.org/10.1016/0025-3227(83)90020-8.

Gilbert, G.K., 1917. Hydraulic-mining Debris in the Sierra Nevada. U.S. Geological Survey Professional Paper 105, 154 pp.

Hoitink, A.J.F., Buschman, F.A., Vermeulen, B., 2009. Continuous measurements of discharge from a horizontal ADCP in a tidal river. Water Resour. Res. 45 (11), W11406.

Hunsaker, L., Curran, C., 2005. Lake Sacramento; Can it Happen Again? Copy Quick & Academy Printing, Grants Pass, Oregon.

Jaffe, B.E., Smith, R.E., Torresan, L.Z., 1998. Sedimentation and Bathymetric Change in San Pablo Bay, 1856–1983. U.S. Geological Survey Open-File Report 98-759.

Jaffe, B.E., Smith, R.E., Foxgrover, A.C., 2007. Anthropogenic influence on sedimentation and intertidal mudflat change in San Pablo Bay, California: 1856–1983. Estuar. Coast. Shelf Sci. 73, 175–187. http://dx.doi.org/10.1016/j.ecss.2007.02.017.

James, A.L., 2004. Decreasing sediment yields in north California: vestiges of hydraulic gold-mining and reservoir trapping. In: Sediment Transfer through the Fluvial System Symposium, Moscow, Russia. IAHS Publ. 288.

James, A.L., 2006. Bed waves at the basin scale: implications for river management and restoration. Earth Surf. Process. Landforms 31, 1692–1706. http://dx.doi.org/10.1002/esp.1432.

James, A.L., 2010. Secular sediment waves, channel bed waves, and legacy sediment. Geogr. Compass 4 (6), 576–598. http://dx.doi.org/10.1111/j.1749-8198.2010.00324.x.

James, A.L., Singer, M.B., 2008. Development of the lower Sacramento Valley flood-control system: historic perspective. Nat. Hazards Rev. 9 (3), 125–135. http://dx.doi.org/10.1061/ASCE1527-698820089:3125.

Jaume, S.C., Sykes, L.R., 1996. Evolution of moderate seismicity in the San Francisco Bay region, 1850 to 1993: seismicity changes related to the occurrence of large and great earthquakes. J. Geophys. Res. 101 (B1), 765–789.

Jay, D.A., Uncles, R.J., Largier, J., Geyer, W.R., Vallino, J., Boynton, W.R., 1997. A review of recent developments in estuarine scalar flux estimation. Estuaries 20 (2), 262–280.

Jay, D., Leffler, K., Degens, S., 2011. Long-term evolution of Columbia River tides. J. Waterway, Port, Coastal, Ocean Eng. 137 (4), 182–191.

Kawanisi, K., Razaz, M., Kaneko, A., Watanabe, S., 2010. Long-term measurement of stream flow and salinity in a tidal river by the use of the fluvial acoustic tomography system. J. Hydrol. 380 (1), 74–81.

Kimmerer, W.J., 2002. Physical, biological, and management responses to variable freshwater flow into the San Francisco estuary. Estuaries 25 (6B), 1275–1290.

Knowles, N., 2002. Natural and management influences on freshwater inflows and salinity in the San Francisco Estuary at monthly to interannual scales. Water Resour. Res. 38 (12), 1289. http://dx.doi.org/10.1029/2001WR000360.

Krone, R.B., 1979. Sedimentation in the San Francisco Bay system. In: Conomos, T.J. (Ed.), San Francisco Bay: The Urbanized Estuary. Pacific Division of the American Association for the Advancement of Science, San Francisco, California, pp. 85–96.

Laudenslayer, W.F., Darr, H.H., 1990. Historical effects of logging on the forests of the cascade and Sierra Nevada Ranges of California. Trans. Western Section Wildlife Soc. 26, 12–23.

Lawson, C.A. et al., 1908. The California earthquake of April 18, 1906, Report of the State Earthquake Investigation Commision. Carnegie Institution of Washington, Washington, D.C.

Lewicki, M., McKee, L., 2010. New Methods for Estimating Annual and Long-term Suspended Sediment Loads from Small Tributaries to San Francisco Bay. IAHS Publication 337, 5 pp.

Logan, T.M., 1872. Report on the physics, hygiene, and thermology of the Sacramento River. In: Proceedings of the Agassiz Institute of Sacramento, CA, K.G. Jefferis & Co., Book and Job Printers, pp. 75–82.

Manning, A.J., Schoellhamer, D.H., 2013. Factors controlling floc settling velocity along a longitudinal estuarine transect. Mar. Geol. 345, 266–280.

McCulloch, M., Fallon, S., Wyndham, T., Hendy, E., Lough, J., Barnes, D., 2002. Coral record of increased sediment flux to the inner Great Barrier Reef since European settlement. Nature 421, 727–730. http://dx.doi.org/10.1038/nature01361.

McKee, L.J., Ganju, N.K., Schoellhamer, D.H., 2006. Estimates of suspended sediment flux entering San Francisco Bay from the Sacramento-San Joaquin Delta, San Francisco Bay, California. J. Hydrol. 323, 335–352.

McKee, L.J., Lewicki, M., Schoellhamer, D.H., Ganju, N.K., 2013. Comparison of sediment supply to San Francisco Bay from watersheds draining the Bay Area and the Central Valley of California. Mar. Geol. 345, 47–62.

Minear, J.T., 2010. The Downstream Geomorphic Effects of Dams: A Comprehensive and Comparative Approach. Dissertation submitted to Department of Landscape Architecture and Environmental Planning, University of California, Berkeley, 207 pp.

Moftakhari, H.R., Jay, D.A., Talke, S.A., Kukulka, T., Bromirski, P.D., 2013. A novel approach to flow estimation in tidal rivers. Water Resour. Res. 49. http://dx.doi.org/10.1002/wrcr.20363.

Muller, G., Forstner, U., 1968. General relationship between suspended sediment concentration and water discharge in the Alpenrhein and some other rivers. Nature 217, 244–245.

Ogden Beeman & Associates, Inc., 1992. Sediment Budget Study for San Francisco Bay. Ogden Beeman & Associates, Inc. Portland, OR and Ray B. Krone & Associates, Inc., Davis, CA

Orton, P.M., Kineke, G.C., 2001. Comparing calculated and observed vertical suspended-sediment distributions from a Hudson River Estuary turbidity

maximum. Estuar. Coast. Shelf Sci. 52 (3), 401–410. http://dx.doi.org/10.1006/ecss.2000.0747.
Pejrup, M., 1986. Parameters affecting fine-grained suspended sediment concentrations in a shallow miro-tidal estuary, Ho Bugt, Denmark. Estuar. Coast. Shelf Sci. 22 (2), 241–254. http://dx.doi.org/10.1016/0272-7714(86)90115-0.
Porterfield, G., 1980. Sediment Transport of Streams Tributary to San Francisco, San Pablo, and Suisun bays, California, 1909–1966. U.S. Geological Survey Water Resources Investigations 91, 64–80.
Powell, T.M., Cloern, J.E., Huzzy, L.M., 1989. Spatial and temporal variability in south San Francisco Bay (USA). I. Horizontal distribution of salinity, suspended sediments, and phytoplankton biomass and productivity. Estuar. Coast. Shelf Sci. 28, 583–597.
Ralston, D.K., Stacey, M.T., 2007. Tidal and meteorological forcing of sediment transport in tributary mudflat channel. Cont. Shelf Res. 27, 1510–1527.
Rose, A.H., Manson, M., Grunsky, C.E., 1895. Report of the Commissioner of Public Works to the Governor of California. State Office, Sacramento, CA.
Ruhl, C.A., Schoellhamer, D.H., Stumpf, R.P., Lindsay, C.L., 2001. Combined use of remote sensing and continuous monitoring to analyze the variability of suspended-sediment concentrations in San Francisco Bay, California. Estuar. Coast. Shelf Sci. 53, 801–812.
Russo, M., 2010. Fact Sheet: Sacramento River Flood Control Project Weirs and Flood Relief Structures. State of California, Department of Water Resources, Division of Flood Management. <http://www.water.ca.gov/newsroom/docs/WeirsReliefStructures.pdf>.
Sassi, M., Hoitink, A., Vermeulen, B., Hidayat, 2011. Discharge estimation from H-ADCP measurements in a tidal river subject to sidewall effects and a mobile bed. Water Resour. Res. 47, W06504. http://dx.doi.org/10.1029/2010WR009972.
Schoellhamer, D.H., 2002. Variability of suspended-sediment concentration at tidal to annual time scales in San Francisco Bay, USA. Cont. Shelf Res. 22, 1857–1866.
Schoellhamer, D.H., 2011. Sudden clearing of estuarine waters upon crossing the threshold from transport to supply regulation of sediment transport as an erodible sediment pool is depleted: San Francisco Bay, 1999. Estuaries Coasts 34 (5), 885–899.
Schoellhamer, D.H., Mumley, T.E., Leatherbarrow, J.E., 2007. Suspended sediment and sediment-associated contaminants in San Francisco Bay. Environ. Res. 105, 119–131.
Sherwood, C.R., Jay, D.A., Harvey, R.B., Hamilton, P., Simenstad, C.A., 1990. Historical changes in the Columbia River estuary. Prog. Oceanogr. 25, 299–352.
Singer, M.B., Aalto, R., James, L.A., 2008. Status of the Lower Sacramento Valley flood-control system within the context of its natural geomorphic setting. Nat. Hazards Rev. 9 (2), 104–115. http://dx.doi.org/10.1061/(ASCE)1527-6988(2008)9:3(104).
Smith, B.J., 1965. Sedimentation in the San Francisco Bay system. In: Proceedings of the Interagency Sedimentation Conference, vol. 970. U.S. Department of Agriculture Miscellaneous Publication, pp. 675–708.
State Engineering Department of California, 1886. Physical Data and Statistics of California; Tables and Memorandum. pp. 405–477.
State of California, 1889. Appendix to the Journals of the State and Assembly of the Twenty-eight Session of the Legislature of the State of California, vol. VII. Sacramento, CA.
Syvitski, J.P., Morehead, M.D., Bahr, D.B., Mulder, T., 2000. Estimating fluvial sediment transport: the rating parameters. Water Resour. Res. 36 (9), 2747–2760. http://dx.doi.org/10.1029/2000WR900133.
Syvitski, J.P.M., Vörösmarty, C.J., Kettner, A.J., Green, P., 2005. Impact of humans on the flux of terrestrial sediment to the global coastal ocean. Science 308 (5720), 376–380. http://dx.doi.org/10.1126/science.1109454.
Talke, S.A., Jay, D.A., 2013. Nineteenth century North American and Pacific tidal data: lost or just forgotten? J. Coastal Res. 29, 118–127. http://dx.doi.org/10.2112/JCOASTRES-D-12-00181.1.
Talke, S.A., Stacey, M.T., 2003. The influence of oceanic swell on flows over an estuarine intertidal mudflat in San Francisco Bay. Estuar. Coast. Shelf Sci. 58, 541–554.
Talke, S.A., Stacey, M.T., 2008. Suspended sediment fluxes at an intertidal flat: the shifting influence on wave, wind, tidal and freshwater forcing. Cont. Shelf Res. 28 (6), 710–725. http://dx.doi.org/10.1016/j.csr.2007.12.003.
Thompson, J., 1957. The Settlement Geography of the Sacramento-San Joaquin Delta, California. PhD Dissertation, Stanford University.
Thrush, S.F., Hewitt, J.E., Cummings, V.J., Ellis, J.I., Hatton, C., Lohrer, A., Norkko, A., 2004. Muddy waters: elevating sediment input to coastal and estuarine habitats. Front. Ecol. Environ. 2, 299–306. http://dx.doi.org/10.1890/1540-9295(2004)002[0299:MWESIT]2.0.CO;2.
US Army Corps of Engineers, 1915. Reports of the Chief of Engineers, US Army 1866–1912; Rivers and Harbors, vol. I. Government Printing Office, Washington, DC.
Vale, C., Sundby, B., 1987. Suspended sediment fluctuations in the Tagus Estuary on semi-diurnal and fortnightly time scales. Estuar. Coast. Shelf Sci. 25 (5), 495–508. http://dx.doi.org/10.1016/0272-7714(87)90110-7.
Wang, H., Yang, Z., Saito, Y., Liu, J.P., Sun, X., Wang, Y., 2007. Stepwise decreases of the Huanghe (Yellow River) sediment load (1950–2005): impacts of climate change and human activities. Global Planet. Change 57 (3–4), 331–354. http://dx.doi.org/10.1016/j.gloplacha.2007.01.003.
Wright, S.A., Schoellhamer, D.H., 2004. Trends in the sediment yield of the Sacramento River, California, 1957–2001. San Francisco Estuary Watershed Sci. 2(2), 14 pp.
Yang, S.L., Belkin, I.M., Belkina, A.I., Zhao, Q.Y., Zhu, J., Ding, P.X., 2003. Delta response to decline in sediment supply from the Yangtze River: evidence of the recent four decades and expectations for the next half-century. Estuar. Coast. Shelf Sci. 57 (4), 689–699. http://dx.doi.org/10.1016/S0272-7714(02)00409-2.
Zervas, C., 2009. Sea Level Variations of the United States 1854–2006. NOAA Technical Report NOS CO-OPS 053, pp. 78.